International Journal of Pharmaceutics 428 (2012) 103–113

Contents lists available at SciVerse ScienceDirect

International Journal of Pharmaceutics

journal homepage: www.elsevier.com/locate/ijpharm

Solid dispersions of itraconazole for inhalation with enhanced dissolution, solubility and dispersion properties

Christophe Duret[a,*], Nathalie Wauthoz[a], Thami Sebti[b], Francis Vanderbist[b], Karim Amighi[a]

[a] Laboratoire de Pharmacie Galénique et de Biopharmacie, Université Libre de Bruxelles, Brussels, Belgium
[b] Laboratoires SMB S.A., 26-28 Rue de la Pastorale, 1080 Brussels, Belgium

ARTICLE INFO

Article history:
Received 5 January 2012
Received in revised form 4 March 2012
Accepted 5 March 2012
Available online 10 March 2012

Keywords:
Itraconazole
Pulmonary aspergillosis
Dry powder for inhalation
Spray-drying
Amorphous
Solid dispersion

ABSTRACT

The purpose of this study was to produce a dry powder for inhalation (DPI) of a poorly soluble active ingredient (itraconazole: ITZ) that would present an improved dissolution rate and enhanced solubility with good aerosolization properties. Solid dispersions of amorphous ITZ, mannitol and, when applicable, D-α-tocopherol polyethylene glycol 1000 succinate (TPGS) were produced by spray-drying hydro-alcoholic solutions in which all agents were dissolved. These dry formulations were characterized in terms of their aerosol performances and their dissolution, solubility and physical properties. Modulate differential scanning calorimetry and X-ray powder diffraction analyses showed that ITZ recovered from the different spray-dried solutions was in an amorphous state and that mannitol was crystalline. The inlet drying temperature and, indirectly, the outlet temperature selected during the spray-drying were critical parameters. The outlet temperature should be below the ITZ glass transition temperature to avoid severe particle agglomeration. The formation of a solid dispersion between amorphous ITZ and mannitol allowed the dry powder to be produced with an improved dissolution rate, greater saturation solubility than bulk ITZ and good aerosol properties. The use of a polymeric surfactant (such as TPGS) was beneficial in terms of dissolution rate acceleration and solubility enhancement, but it also reduced aerosol performance. For example, significant dissolution rate acceleration ($f_2 < 50$) and greater saturation solubility were obtained when introducing 1% (w/w) TPGS (mean dissolution time dropped from 50.4 min to 36.9 min and saturation solubility increased from 20 ± 3 ng/ml to 46 ± 2 ng/ml). However, the fine particle fraction dropped from $47 \pm 2\%$ to $37.2 \pm 0.4\%$. This study showed that mannitol solid dispersions may provide an effective formulation type for producing DPIs of poorly soluble active ingredients, as exemplified by ITZ.

1. Introduction

Active pharmaceutical ingredients (APIs) can be administered to the lung either as a solution or a suspension using nebulizer or pressurized metered dose inhalers or as a dry powder using dry powder inhalers. Pressurized metered dose inhalers and nebulizer medicines are losing interest due to their specific weaknesses, and dry powder for inhalation (DPI) medicines are currently the focus of research development in the pulmonary delivery field. The administration of an API-based dry powder formulation to the lung involves several specific considerations that can limit the design and development of a DPI medicine. Indeed, the powder must present a maximum proportion of particles with an aerodynamic diameter (d_{ae}) between 0.5 and 5 μm after being emitted from the dry powder inhaler by the inspiratory flow. This d_{ae} limitation is required because only particles within this size range will deposit in the lung. Particles over 5 μm will be stopped in the upper airways by inertial impaction, and particles smaller than 0.5 μm could be exhaled during expiration. The formulation strategies must maximize this proportion of fine particles by offering suitable particle size distributions and good flow and dispersion properties using excipient suitable for pulmonary administration (Pilcer and Amighi, 2010). Additionally, to be marketed, the manufacturing process must be easily scalable. For this purpose, the

Abbreviations: API, active pharmaceutical ingredient; CI, Carr compressibility index; d_{ae}, aerodynamic diameter; DPI, dry powder for inhalation; f_2, the similarity factor; FPD, fine particle dose; FPF, fine particle fraction; GRAS, generally recognized as safe; HPLC-UV, high performance liquid chromatography coupled to ultra-violet detection; HSM, hot stage microscopy; ITZ, itraconazole; MTDSC, modulated temperature differential scanning calorimetry; MDT, mean dissolution time; MsLI, multi-stage liquid impinger; NGI, next generation impactor; pMDI, pressurised metered dose inhaler; SD, solid dispersion; SEM, scanning electron microscopy; TPGS, tocopherol polyethylene glycol 1000 succinate; XRPD, X-ray powder diffraction.

* Corresponding author at: Laboratory of Pharmaceutics and Biopharmaceutics, Faculty of Pharmacy, ULB, Boulevard du Triomphe - CP207 Campus de la Plaine, B-1050 Brussels, Belgium. Tel.: +32 2 650 53 31; fax: +32 2 650 52 69.
E-mail address: cduret@ulb.ac.be (C. Duret).

0378-5173/$ – see front matter © 2012 Elsevier B.V. All rights reserved.
doi:10.1016/j.ijpharm.2012.03.002

production process should be as simple as possible using equipment and techniques that are readily transposable to an industrial scale.

More particularly, many existing APIs and an increasing number of new ones are often poorly water-soluble drugs. Approximately 40% of the drugs on the market and 70–90% of the drugs currently in research and development are poorly soluble in water (Zhang et al., 2011). Drug insolubility, regardless of the administration route, commonly generates bioavailability or efficacy problems. In the inhalation field, DPI formulations based on a poorly water-soluble drug should be able to provide a powder presenting a high fine particle fraction (FPF) after emission from a dry powder inhaler and to improve drug wettability, solubility and dissolution. Indeed, poor drug dissolution and wettability could induce lung irritation and therefore local side effects (Tran et al., 2000; Jones and Neef, 2012). Having a solubility and dissolution rate that are too low could also result in excessive non-absorptive clearance (macrophage phagocytosis and/or mucociliary clearance) of solid particles, leading to a rapid dose reduction in the lung (Mobley and Hochhaus, 2001). Because the activity and/or absorption of a drug are limited by the number of its molecules that are dissolved, accelerating a drug's dissolution rate could be necessary to overcome these clearance mechanisms and optimize the drug's efficacy.

Different techniques exist to increase drug dissolution and/or solubility, such as complexation within cyclodextrins (Loftsson and Brewster, 2010), particle size reduction (Van Eerdenbrugh et al., 2010), crystal engineering (Blagden et al., 2007; Hickey et al., 2007) and even the formation of a lipid-based delivery system (Porter et al., 2007). However, these strategies often require the use of specific excipients to achieve the final dissolution enhancement effect or the desired particle formation. Ideally, inhaled excipients should be chemically and physically stable and inert to the API and should not exhibit harmful effects, especially on the respiratory tract. Knowing that (i) the number of authorized inactive ingredients that can be used in the development of inhalable pharmaceutical products is quite limited (http://www.accessdata.fda.gov/scripts/cder/iig/index.cfm, 2011) and (ii) the documentation on the safety profile of potential excipients intended to be administered by the pulmonary route is usually incomplete (Pilcer and Amighi, 2010), these realities considerably reduce formulation possibilities in the development of poorly water-soluble drug-based DPIs.

Regarding problems underlying above, a formulation strategy must be set up to allow poorly water-soluble active ingredient based DPI to offer (i) a high lung deposition, (ii) an improved solubility and dissolution profile and (iii) an acceptable safety profile, in regards with excipients used. The aim of this study was to evaluate one DPI formulation strategy consisting of the formation of a poorly water-soluble drug based solid dispersions (SDs) produced by a spray-drying process to meet these needs. Indeed, the formation of a SD between a poorly water-soluble drug particle and a hydrophilic inactive ingredient that is generally recognized as safe (GRAS), such as a carbohydrate, could be an effective method of increasing the drug dissolution rate and saturation solubility while providing good aerosol and flow properties. In SD formulations, the drug dissolution rate could be improved by reducing the drug particle size to almost a molecular level and by modifying the drug crystalline state to generate a completely or partially amorphous state, both of which may increase drug saturation solubility (Serajuddin, 1999).

Itraconazole (ITZ) has previously shown interesting potential for treating pulmonary invasive fungal infection *via* inhalation (nebulization) (Hoeben et al., 2006) and was chosen in this report as a model of an insoluble API. This molecule presents very low saturation solubility (approximately 1 ng/mL at neutral pH and 4 μg/mL at pH 1) and a log *P* of 6.2. Due to its low solubility and high permeability, ITZ is a class II drug molecule according to the biopharmaceutical classification system (Amidon et al., 1995). Its low dissolution rate and saturation solubility could therefore be a limiting factor in its efficacy (Yang et al., 2010). Mannitol was chosen as the SD hydrophilic agent for its various interesting physicochemical properties and its safety profile after inhalation. Indeed, this excipient is currently recognized as safe for inhalation (Daviskas et al., 2010) and provides a sweet taste when in contact with mouth mucosa, which tends to improve patient compliance. Additionally, this carbohydrate is one of the less hygroscopic sugars, preventing excessive reuptake of water by powders during storage. Consequently, it prevents particle agglomeration and aggregation arising from the appearance of additional capillary forces between particles, which decrease DPI aerosol performance. Moreover, mannitol was also selected instead of the more classic lactose or sorbitol, which are generally used in inhalation, because of its potential to form a SD with improved solubility (Vasconcelos et al., 2007) and its ability to stabilize an amorphous drug compound (Lian, 2001), which may be both beneficial in our formulation strategy. The addition of TPGS to the formulation composition was also evaluated. TPGS is a surfactant that is potentially eligible for pulmonary administration because of its good performance and safe potential in the formulation and administration of pulmonary formulations (Yan et al., 2007; Shah and Banerjee, 2011).

2. Materials and methods

2.1. Materials

Raw ITZ was purchased from Hetero Drugs Ltd. (Hyderabad, India). This powder was micronized by jet milling (volume mean diameter, 3.5 μm; 90% of particles below 6.2 μm). Sodium lauryl sulfate and TPGS were purchased from Sigma–Aldrich (Brussels, Belgium). Pearlitol PF® (mannitol) was donated by Roquette Frères (Lestreme, France). Dipalmitoylphosphatidylcholine (DPPC) was purchased from Lipoid® (Ludwigshafen, Germany). All the solvents were analytical grade.

2.2. Methods

2.2.1. Production of SD formulations

The theoretical compositions of the formulations (A1, A2, A3, A4, A5 and A6) before and after spray-drying are described in Table 1. First, the different ingredients were dissolved under magnetic stirring (600 rpm) in a hydro-alcoholic solution of isopropanol (80%) and water (20%) heated to 70 °C. Then, the solutions containing the hydrophilic agent (mannitol), the API (ITZ) and, in some solutions, the TPGS as a surfactant were spray-dried using a Büchi Mini Spray-Dryer B-191-a (Büchi Laboratory Techniques, Flawil, Switzerland) to produce the DPI formulations in a one-step process. For each assay, the following spray-drying conditions were used: spraying air flow, 800 l/h; drying air flow, 35 m^3/h; solution feed rate, 2.7 g/min; and nozzle size, 0.5 mm. The inlet and resulting outlet spray-dryer temperatures for each formulation are reported in Table 1.

2.2.2. Particle size analysis

The particle sizes were measured using a laser diffraction based apparatus (Malvern Mastersizer 2000) equipped with a Sirocco® dry dispersion system (Malvern Instruments Ltd., Malvern, United Kingdom). A pressure of 4 bar and a feed rate vibration of 50% were used during the measurements. The very drastic dispersion conditions applied to the sample by this technique allow particle size distribution measurement of almost totally disaggregated powder particles. Particle size distributions were calculated using a refractive index of 1.61 for bulk ITZ and 1.48 for all dry powders. The

Table 1
Theoretical composition of formulations (A1, A2, A3, A4, A5 and A6) before and after spray-drying and the inlet and generated outlet spray-dryer temperatures used during the process.

Formulations								
Composition								
	Spray-dried solutions			Final dried forms			Spray-dryer temperatures	
	ITZ (%, w/v)	Mannitol (%, w/v)	TPGS (%, w/v)	ITZ (%, w/w)	Mannitol (%, w/w)	TPGS (%, w/w)	Inlet temperature	Outlet temperature
A1	0.56	1	–	35.9	64.1	–	90	55
A2	0.56	1	–	35.9	64.1	–	100	60
A3	0.56	1	–	35.9	64.1	–	110	65
A4	0.56	1	–	35.9	64.1	–	120	70
A5	0.56	1	0.056	34.65	61.88	3.47	90	55
A6	0.1	0.9	0.01	9.90	89.11	0.99	90	55

results were expressed in terms of $D[4,3]$, $d(0.5)$ and $d(0.9)$, which are the volume mean diameter and the sizes in microns at which 50% and 90% of the particles are smaller than the rest of the distribution, respectively. All samples were analyzed in triplicate and are expressed as a mean ± standard deviation.

2.2.3. Drug content determination

The drug content of the dry powders was determined as follows.

For each formulation, 5 samples of an exactly weighed quantity of powder were dissolved in a volumetric flask containing the dilution phase (50:50, v/v of acetonitrile and phosphate buffer) and then sonicated for 20 min. The amount of ITZ in this solution was quantified using the high performance liquid chromatography coupled to ultra-violet detection (HPLC-UV) method described in Section 2.2.11. The average content (wt%) and the standard deviation were calculated from these 5 analyses. Relative errors were calculated based on the calculated average drug contents and expected theoretical content.

2.2.4. Powder flowability evaluation

Powder flowability was evaluated by calculating the Carr compressibility index (CI) or "Carr's index" as described in European Pharmacopeia 7.2. A pre-weighed quantity of dry powder was placed in a graduated 10 ml cylinder. The apparent volume occupied by the powder was then noted before and after the application of 1000 taps to the cylinder using a tap density tester (Stampfvolumeter, STAV 2003, Jel, Germany).

2.2.5. Scanning electron microscopy (SEM)

The morphology of each dry powder was studied using a field emission scanning electron microscope (Philips XL30 ESEM-FEG; FEI, Eindhoven, The Netherlands). The acceleration voltage during observation ranged from 5 keV to 25 keV, depending on the samples. Images were taken randomly at magnifications ranging from 1000× to 10,000×. Prior to imaging, the samples were spread on a carbon adhesive band and then coated with gold at 40 mA for 90 s at 6×10^{-2} mbar under argon to a thickness of approximately 15–20 nm.

2.2.6. Hot stage microscopy (HSM)

The DPI samples were placed on a plate heated from 50 °C to 90 °C per steps of 5 °C maintained during 60 min (per increment) follow by a continuous heating from 90 to 180 °C at a rate of 5 °C/min. Samples were heated on a Linkam hot-stage THMS unit (Linkam Scientific Instruments, Tadworth, England) using a universal temperature programmer (THMS 600, Linkam Scientific Instruments, Tadworth, England). During the scanning, a TK-C1381 digital camera (JVC, Yokohama, Japan) connected to an optical microscope (Olympus BX60, Olympus Optical Co., Tokyo, Japan) was used to photograph the thermal events. The magnification used to take the pictures was 200×. A polarizer was placed just before the light source to determine the crystalline phases in the samples.

2.2.7. Modulated temperature differential scanning calorimetry (MTDSC)

The thermal response of each powder was analyzed using MTDSC (Q 2000; TA Instruments, Zellik, Belgium). A 2–3 mg sample was exactly weighed in a low-mass aluminum hermetic pan. Runs were conducted from 25 °C to 185 °C at a heating rate of 5 °C/min with a modulation of ±0.80 °C every 60 s.

2.2.8. X-ray powder diffraction (XRDP)

The X-ray powder diffraction pattern for each dry powder was analyzed using a diffractometer (Siemens D5000, Munich, Germany) equipped with a mounting for Bragg-Brentano reflection that was connected to a monochromator and a DIFFRACplus channel program. Measurements were conducted at room temperature using Cu Kα radiation at 40 mA and 40 kV, with an angular 2θ increment of 0.02 °/s and a counting speed of 1.2 s per step. A rotation of 15 rpm was applied to the samples.

2.2.9. Drug dissolution profiles and saturation solubilities

Size separation pretreatments using a multi-stage impactor were applied to the different dry powders to assess the drug dissolution profiles and the saturation solubilities on a DPI respirable fraction ($d_{ae} < 5$ μm).

For drug dissolution tests, we used a recent Copley® dissolution system (Copley Scientific, Nottingham, England) specifically developed for DPI release profile evaluations (Wauthoz et al., 2010). This dissolution system is composed of a modified next generation impactor (NGI) containing a dissolution cup on which a 50 mm removable insert can be fitted. This system can be placed on each stage of the NGI to collect particles of the dose emitted from the inhaler that present a specific aerodynamic size range. Dose actuation was realized once per insert at a flow rate of 60 L/min for 4 s, which allowed recovery on the insert (placed on stage 3 of the NGI) of particles presenting an aerodynamic diameter between 2.82 μm and 4.46 μm. The device used for powder dispersion was an Axahaler® (SMB, Brussels, Belgium). This device is a low-resistance capsule-based device containing a no. 3 HPMC capsule filled with a quantity of dry powder that generated a deposited dose on the insert of approximately 600 μg of ITZ after actuation.

To evaluate the drug saturation solubility kinetics, we collected the same aerodynamic particle size range as for the drug dissolution test. However, instead of using a removal insert, the powder was collected from the NGI cup and was then introduced in bulk into the dissolution vessel.

2.2.9.1. Drug dissolution test in sink conditions. The dissolution tests were not realized at lung physiologic pH because *in vitro* sink conditions could not be reached at this pH. Indeed, because ITZ is a

weak base (p*Ka* = 3.4), its solubility at physiologic pH is extremely low (~8 ng/ml) (Yang et al., 2010). Because the dissolution tests were mainly used to discriminate between the dissolution profiles of the developed formulations, we decided to work in acidic pH to reach sink conditions. We chose a dissolution medium that had been previously used for ITZ pulmonary formulation dissolution tests (McConville et al., 2006). This solution was composed of water at pH 1.2 (HCl 0.063N) and 0.3% sodium lauryl sulfate. Once aerosolized particles were deposited on the removable insert by inertial impaction, a polycarbonate membrane (0.4 μm diameter pores) (Millipore, Brussels, Belgium) was placed on the top of the insert and was sealed with the sealing ring of a Copley® dissolution system. The sealed insert was then placed in the bottom of a dissolution vessel of a paddle apparatus (USP 33 type 2 apparatus, Erweka DT6, Heusenstamm, Germany) to conduct the dissolution tests. The dissolution conditions included the following: (i) a paddle rotation speed of 75 rpm, (ii) a dissolution medium volume of 300 ml and (iii) a dissolution medium temperature maintained at 37.0 ± 0.2 °C. The dissolution tests were carried out in triplicate for each formulation, and the percentages of dissolved ITZ were determined by HPLC-UV analysis (Section 2.2.11) at pre-selected time intervals up to 180 min after insert introduction in the dissolution media. These ITZ quantities were deposited on an insert after dose actuation and allowed the dissolution tests to be carried out in sink conditions. The maximum drug concentration in solution was 3.3 μg/ml, whereas the saturation solubility of ITZ in this medium was >800 μg/ml. After 180 min, the sealed insert was removed from the dissolution vessel and washed with an exact volume of dilution phase for quantification of the undissolved fraction.

2.2.9.2. Drug saturation kinetic evaluation in "physiological" conditions. The formulations' saturation solubility kinetics were determined to evaluate their potential to provide supersaturated solutions in a medium that is similar to that encountered into the lung. Moss (1979) developed a dissolution medium called "simulated lung fluid" (SLF), which was described as close to lung surfactant in ion composition and pH. However, we observed that the pH of SLF increased rapidly (from 7.2 to 8 within 2 h) due to its poor buffering power. Because the solubility of ITZ is strongly influenced by pH, this dissolution medium was not appropriate. Instead of the SLF, we used a physiological buffered solution described in the European Pharmacopoeia 7.2 (pH adjusted to 7.2). DPPC (0.02%, w/v) was added to this solution, as described by Son and McConville (2009), to simulate the wetting enhancer effect of lung surfactant (Pham and Wiedmann, 2001). The "physiological" solution was composed (w/v) of 0.8% sodium chloride, 0.02% potassium chloride, 0.01% calcium chloride, 0.01% magnesium chloride, 0.318% disodium hydrogen phosphate and 0.02% potassium dihydrogen phosphate. The tests were carried out using a USP 33 type II (paddle method) dissolution apparatus (Distek Inc., North Brunswick, NJ, USA) equipped with 100 ml glass dissolution vessels and small rotating paddles (rotating speed set at 200 rpm). The medium temperature was maintained at 37.0 ± 0.2 °C throughout the test. An excess of powder formulation (d_{ae} between 2.82 and 4.46 μm) corresponding to 1 mg of ITZ was pre-wetted in 2 ml of dissolution medium (4 °C) by vortex shaking for 5 s and introduced into dissolution vessels to achieve saturation kinetic. Then, 2 ml samples were withdrawn after 2, 5, 10, 25, 45, 60, 75, 90, 120, 180, 720 and 1440 min and directly filtered through 0.2 μm filters to avoid quantifying undissolved particles. Samples were then reconstituted with acetonitrile for HPLC-UV quantification.

2.2.10. Aerodynamic behavior evaluation

The aerosolization efficiency of the DPI formulations was evaluated using a multi-stage liquid impactor (MsLI) (Copley Scientific, Nottingham, England) following the operating procedure described for the aerodynamic assessment of fine particles in European Pharmacopoeia 7.2. A flow rate (adjusted to a pressure drop of 4 kPa) of 100 L/min was applied for 2.4 s throughout the Axahaler® inhaler device (SMB, Brussels, Belgium) for each dose actuation. The flow rate was measured using a DFM3 flow meter (Copley Scientific, Nottingham, England). A quantity of formulation corresponding to approximately 2.5 mg of ITZ was accurately weighed into a size 3 HPMC capsule (Capsugel, Colmar, France), which was placed into the loading chamber of the Axahaler® inhaler. The device was inserted on a mouthpiece adapter, which was connected to the induction port (simulating the throat) of the MsLI. The flow rate was applied throughout the whole system for dose actuations. One test utilized three capsules. The aerosol performances of the different formulations were assessed by determining the FPF (express in % of the nominal dose) and the mass median aerodynamic diameter (MMAD) on the basis of the results of the impaction tests. The FPF represents the percentage of particles with a d_{ae} of less than 5 μm. This procedure was carried out in triplicate for each formulation. The emitted dose corresponds to the dose of drug that was recovered from the induction port and the different parts of the MsLI during the tests.

2.2.11. ITZ determination—HPLC-UV method

ITZ determination was carried out using an HP 1200 series chromatographic system (Agilent Technologies, Belgium) equipped with a binary pump, an auto sampler and a diode array detector with a detection wavelength set at 263 nm. The separations were performed on a base-deactivated reverse-phase Purospher® Star RP-18 column (Merck Chemicals, Belgium). The mobile phase (acetonitrile-phosphate buffer, pH 6.4 (60:40, v/v)) was run at a flow rate of 1 ml/min. Samples were diluted in the dilution phase, which comprised acetonitrile and phosphate buffer, pH 6.4 (50:50, v/v). The volume injected was 100 μl, the temperature was set at 25 °C, and the analysis time was 8.2 min.

2.2.12. Statistical analysis

Two kinetic model-independent approaches, the determination of the similarity factor (f_2) and the mean dissolution time (MDT) (Polli et al., 1997), were used to compare dissolution profiles. f_2 values greater than 50 were used to indicate that two dissolution profiles were similar. Inversely, f_2 values below 50 indicated that there were significant differences between two dissolution profiles.

3. Results and discussion

3.1. Development of formulations

Classic DPI formulations consist of a blend of micronized API with a larger grained carrier (generally lactose) (Pilcer et al., 2011), which allows for good dispersion and deep penetration of the API in the lung but does not enhance solubility. Instead of producing a blended formulation, we tried to prepare microparticles of mannitol wherein API (ITZ), in an amorphous state if possible, was dispersed to obtain a dry powder with good flow properties, high FPF and with improved API dissolution rate and/or saturation solubility. We used spray-drying to produce a SD-based dry powder from a solution in which the API and the hydrophilic excipient (present in a greater quantity than the API, see Table 1) were dissolved. However, ITZ is poorly soluble in most solvents except chlorinated solvents, such as dichloromethane, in which mannitol is insoluble. Preliminary studies allowed us to find a method to simultaneously dissolve the ITZ and hydrophilic excipients. Adding 20% water to isopropanol to form a hydro-alcoholic solution that was heated to 70 °C allowed ITZ and the inactive ingredient(s) to be easily dissolved under moderate magnetic stirring. The dried

particles were obtained thereafter by spray-drying. The process yield was between 40% and 60%.

3.2. Physicochemical properties (crystalline profile–drug content)

Fig. 1 displays the X-ray diffractograms of raw ITZ, raw TPGS, spray-dried mannitol, a physical mixture (PM) of components contained in all formulations and the different SD formulations (A1, A2, A3, A4, A5, and A6). SD formulations did no show specifics diffraction peaks of crystalline ITZ while the PM exhibited it (Fig. 1). This suggested that ITZ was not in crystalline state in the spray-dried formulations. The different diffraction peaks found in the SD formulations corresponded to the mannitol (Fig. 1). The MTDSC analysis revealed thermal events specific to amorphous glassy ITZ (Six et al., 2001) for the SD formulations which validated ITZ amorphous state suggested by the PXRD results. These thermal events are illustrated in Fig. 2 for formulation A1 and are identified by the glass transition at 49 °C and the two typical endotherms at approximately 70 °C and 80 °C, which correspond to the formation and chiral rearrangement of liquid mesotropic mesophases that are characteristic of glassy ITZ. These thermal events were followed by recrystallization phenomena between 100 and 120 °C and by the melting of the re-crystallized ITZ and mannitol, which both melt at the same temperature (i.e., 162–164 °C). The thermograms for all SD formulations showed thermal events specific to glassy ITZ, except for formulation A6 (Fig. 2), which contained only ~10% (w/w) ITZ (*vs.* ~35% for the other formulations). This drug content was probably too low to detect these thermal events by MTDSC analysis. However, the lack of any ITZ diffraction peak on the X-ray diffractograms (Fig. 1) allowed us to assume that ITZ would also be present in a glassy amorphous state in formulation A6. This assumption was confirmed by the detection of crystalline ITZ X-ray diffractions peaks in a control blend of raw crystalline ITZ (10%, w/w) and spray-dried mannitol (data not shown). In particular, MTDSC thermogram and X-ray diffractograms of the formulations with TPGS (formulations A5 and A6) showed no evidence of crystalline TPGS. However, the concentration of this excipient in these SD formulations was very low (approximately 1% or 3.5%) and probably below the detection limit of the two techniques. Most of the TPGS is likely amorphous after the spray-drying process (Goddeeris et al., 2008) in formulations A5 and A6.

The determination of actual and expected values of ITZ content in the dry powders is summarized in Table 2. The actual values were used to calculate the exact dose of ITZ used during the dissolution and impaction tests. The measured ITZ contents were very close to those expected. Relative errors were between −0.26% and −3.9%, suggesting that ITZ was homogenously dispersed in the particles. However, because ITZ is highly hydrophobic, it is not miscible with mannitol, and the typical thermal events of ITZ mesotropic mesophases that were detected by MTDSC revealed that ITZ must be dispersed in the DPI particles as free glassy clusters, as previously reported by Six et al. (2003).

3.3. Physical transformations and aerosol performance

The particle size analyses carried out by laser diffraction are summarized in Table 3. The particle size measurement of the dried formulations showed that the inlet temperature of the spray-dryer seemed to broadly influence the particle size of the produced particles. Considerable increases in particle size were observed for the formulations that were spray-dried at an inlet temperature above 90 °C (formulations A2, A3 and A4; Table 3). These formulations did not show a particle size distribution that was appropriated for pulmonary administration because individualized particles should present a d_{ae} below 5 μm to penetrate into the lung (Schulz, 1998). For these reasons, formulations that were spray-dried at an inlet temperature higher than 90 °C were not investigated further. However, we suggest an explanation for this increase in particle size. The higher the inlet temperature was, the larger the particles formed by spray-drying were. The D[4,3] value increased from 1.0 μm at 90 °C to 34 μm at 120 °C (with a D[4,3] of 10 μm at 100 °C and 23 μm at 110 °C), whereas the d(0.5), expressing the middle of the distribution, only varied from 0.74 μm at 90 °C to 5.8 μm at 120 °C. The difference in particle size between these formulations can be seen easily in Fig. 3, which shows SEM pictures of the different DPI formulations. The smaller increase in d(0.5) as a function of the temperature compared to the more considerable increase in D[4,3] and d(0.9) (Table 3) can be explained by the formation of additional larger particles when the inlet temperature increased, while the major part of the "original-sized" particles remained. ITZ was found in the formulations in a particular amorphous glassy state that has the characteristic of forming liquid crystals at a temperature of approximately 70 °C. We therefore hypothesized that the latency period of the dried powder in the powder collector (temperatures of 60 °C, 65 °C and 70 °C for formulation A2, A3 and A4, respectively) during the spray-drying procedure was long enough to form ITZ liquid crystals at a temperature above its glass transition temperature (48–50 °C). These crystals then solidified upon cooling to create compact agglomerates. To confirm this hypothesis, spray-dried formulation A1 was analyzed by HSM to simulate the temperature conditions encountered in the powder collector during spray-drying. Fig. 4 shows pictures taken at different temperatures with and without the polarizer. After being kept at 60 °C for 15 min, the sample exhibited visual modifications (Fig. 4C and D, white circles) that were accentuated at 80 °C and even more so at 90 °C (data not shown). These modifications were explained, as previously seen, by the formation of liquid crystals of ITZ. At these temperatures, the liquefaction of the solid entrapped glassy ITZ in the mannitol microparticles induced those visual modifications. These liquid crystals in formulation A1, as revealed by MTDSC analysis, were assumed to recrystallize at temperatures up to 100 °C. Indeed, these newly formed crystals became visible under polarized light starting at 105 °C (data not shown). Their intensity reached a maximum at 120 °C, indicating an increase in the crystalline fraction (Fig. 4F). Subsequently, during spray-drying at an inlet temperature fixed above or equal to 100 °C, a generated outlet temperature equal to or above 60 °C induced the liquid transition of ITZ, which caused particle agglomeration upon cooling because of the reversibility of this liquid transition (Six et al., 2001). For an inlet temperature of 90 °C (formulation A1: outlet temperature, 55 °C), discrete particles were formed (Fig. 3A), as observed by SEM, while for an inlet temperature of above 100 °C (formulation A2: outlet temperature, 60 °C), these particles fused together and formed linked spheres (Fig. 3B), precluding re-dispersion. This particle agglomeration was exacerbated for inlet temperatures above 100 °C, probably due to higher outlet temperatures, which made the liquid transition easier and induced the formation of severe agglomerates (Fig. 3C).

The use of TPGS (formulations A5 and A6) increased the particle size in comparison with the formulation without TPGS (formulation A1) that was spray-dried at the same temperature. Formulations A5, A6 and A1 (the only one without TPGS) exhibited a d(0.5) of 4.6, 1.6 and 0.7 μm, respectively. Formulation A5, containing 3.47% (w/w) TPGS, showed a larger particle size than formulation A6, containing only 0.99% TPGS. As shown in pictures taken by SEM (Fig. 3D and E), despite their low concentrations of TPGS, these two formulations consist of irregular particles sticking to each other that are not very well distinguished and have wrinkled surfaces. The waxy, sticky property of TPGS may contribute to these characteristics. Moreover, TPGS has a low melting point (between 30 and 40 °C) that could induce particle softening or melting during the spray-drying process (outlet temperatures of 55 °C), which may induce

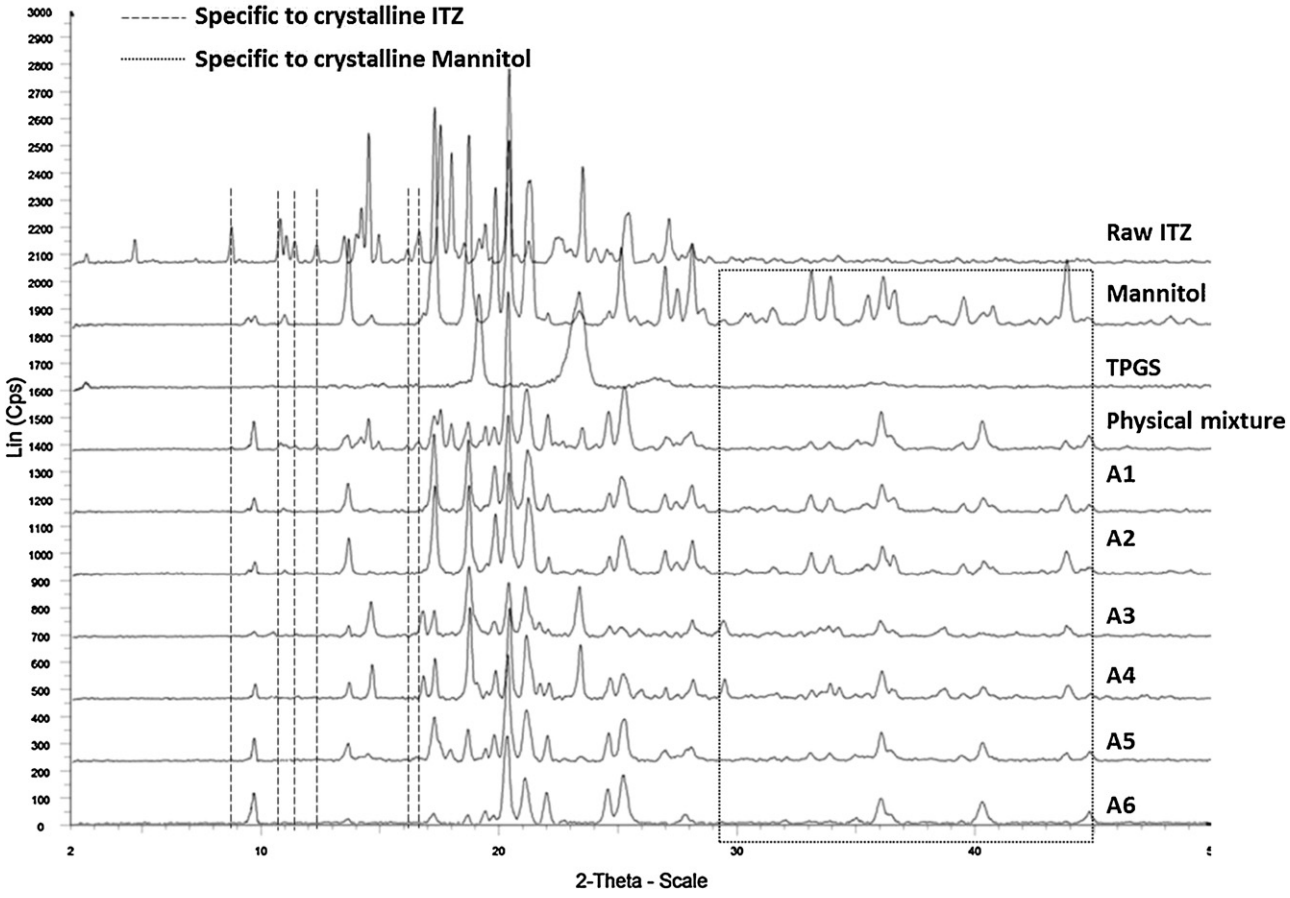

Fig. 1. X-ray diffractograms of raw ITZ, spray-dried mannitol, TPGS, physical mixture of formulations components and the SD formulations (A1, A2, A3, A4, A5 and A6).

increases in particle size and irregularities. The particle irregularity of formulations A5 and A6 may be explained by the surface accumulation of TPGS (Kawakami et al., 2010). This surface accumulation could be elucidated by the active surface properties of TPGS and by its high molecular weight (1.5 kDa), which reduces its diffusion coefficient. During droplet evaporation, surfactants are assumed to be adsorbed at the liquid-air interface due to the tendency of low diffusion polymers to remain outside the particles (Chang and Franses, 1995). Higher TPGS concentrations lead to greater surface accumulation on the particles. This pattern with TPGS probable melting may explain why formulation A5 exhibited greater particle size than formulation A6. However, according to the laser diffraction results, more than 50% and 90% of the particles in these two formulations, respectively, had a diameter below 5.0 μm. This

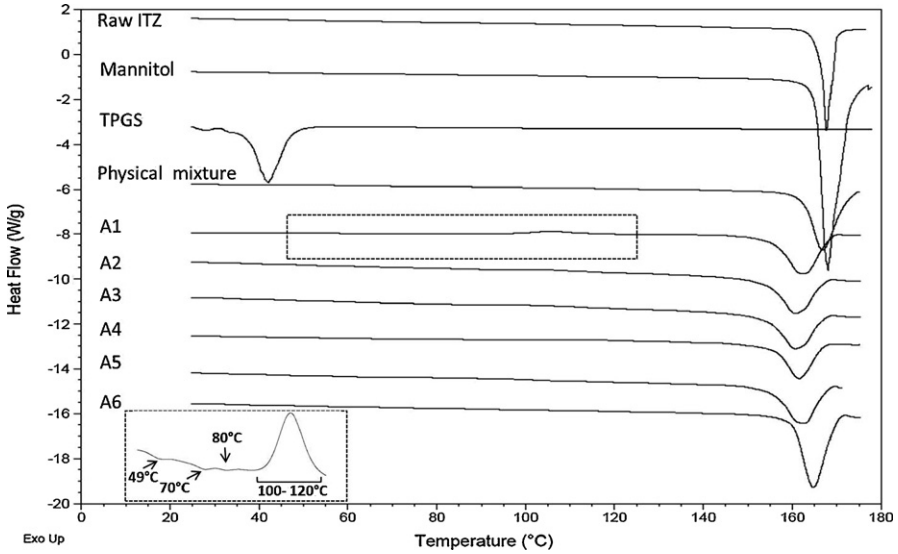

Fig. 2. Heating curves obtained by MTDSC of raw ITZ, spray-dried mannitol, TPGS, physical mixture of formulations components and the SD formulations (A1, A2, A3, A4, A5 and A6) (exothermic events move upward). The dashed boxes show the characteristic thermal transition of glassy ITZ.

Table 2
Drug content and flow properties of DPI formulations A1, A5 and A6 and raw ITZ. Drug concentrations were measured by HPLC-UV. Flow properties were evaluated by calculating the Carr's index.

Drug content					Flow properties			Dissolution characteristics	
Sample	Measured ITZ content (wt%)	Coefficient of variation (%)	Expected ITZ content (wt%)	Relative error (%)	Bulk density	Tapped density	Carr's index	Mean dissolution time (min)	Saturation solubility (ng/ml)
A1	34.5 ± 0.6	1.64	35.9	−3.9	0.277	0.376	26.3	50.4	20 ± 3
A5	34.6 ± 0.8	2.47	34.65	−0.26	0.216	0.270	20.0	49.6	21 ± 3
A6	9.8 ± 0.3	3.18	9.99	−1.45	0.161	0.207	22.2	37.9	46 ± 2
Raw ITZ	100.1 ± 0.5	0.5	100	0.1	0.196	0.353	44.4	62.1	ND (<10 ng/ml)

Table 3
Particle size characteristics of DPI formulations. $D[4,3]$, $d(0.5)$ and $d(0.9)$ (in μm; mean ± S.D., $n = 3$) were measured by laser diffraction using a Malvern Mastersizer 2000 equipped with a dry dispersion unit. The aerodynamic behavior of formulations (A1, A5 and A6) was assessed by determining the FPF, expressed as a percentage of the nominal dose, using an MsLI at 100 l/min for 2.4 s with an Axahaler® (mean ± S.D., $n = 3$).

	A1	A2	A3	A4	A5	A6
Laser particle size distribution						
$D[4,3]$ (μm)	1.00 ± 0.04	10 ± 4	23 ± 5	34 ± 3	11.5 ± 4.4	1.86 ± 0.12
$d(0.5)$ (μm)	0.74 ± 0.01	5.1 ± 0.4	5.5 ± 0.4	5.8 ± 0.5	4.6 ± 0.1	1.6 ± 0.1
$d(0.9)$ (μm)	1.8 ± 0.1	29 ± 15	51 ± 18	119 ± 10	24 ± 12	3.6 ± 0.3
Aerodynamic evaluation (MsLI)						
FPF (%)	47 ± 2	–	–	–	16 ± 2	37.2 ± 0.4
ED (%)	53 ± 2	–	–	–	86 ± 6	82 ± 1
MMAD (μm)	1.61 ± 0.05	–	–	–	4.5 ± 0.6	3.0 ± 0.1

diameter corresponds to the upper size limit required for optimal deep lung deposition.

The CI is an indication of the flowability of a powder. A CI greater than 25% is considered to be an indication of poor flowability. The CI values of the different formulations are reported in Table 2. Formulations A5 and A6 exhibited the best flow properties (CI of 20.0% and 22.2%, respectively), and formulation A1 showed the worst flowability (CI of 26.3%), although this value was much better than the CI of raw ITZ (44.4%).

The *in vitro* pulmonary deposition patterns of SD formulations and the percentage of the ITZ nominal dose recovered at each stage of the impinger during impactions tests are shown in Fig. 5. The drug recoveries from the assays of all formulations were within 85–95% of the loaded dose, which was in the range recommended by European Pharmacopeia 7.2. The formulation without TPGS (formulation A1) presented the highest FPF (i.e. particles presenting a $d_{ae} < 5$ μm), which indicates the best aerosol performance. The addition of TPGS (formulations A5 and A6) considerably enhanced the particle sizes as measured by laser diffraction, and therefore the aerodynamic diameters which increase the percentage stopped in the upper stages of the impactor (i.e. in the induction port, stage 1 and stage 2). Indeed, formulation A5 and A6 presented a $D[4,3]$ of 11.5 ± 4.4 μm and 1.86 ± 0.12 μm, a MMAD of 4.5 ± 0.6 μm and 3.0 ± 0.1 μm and a percentage of powders

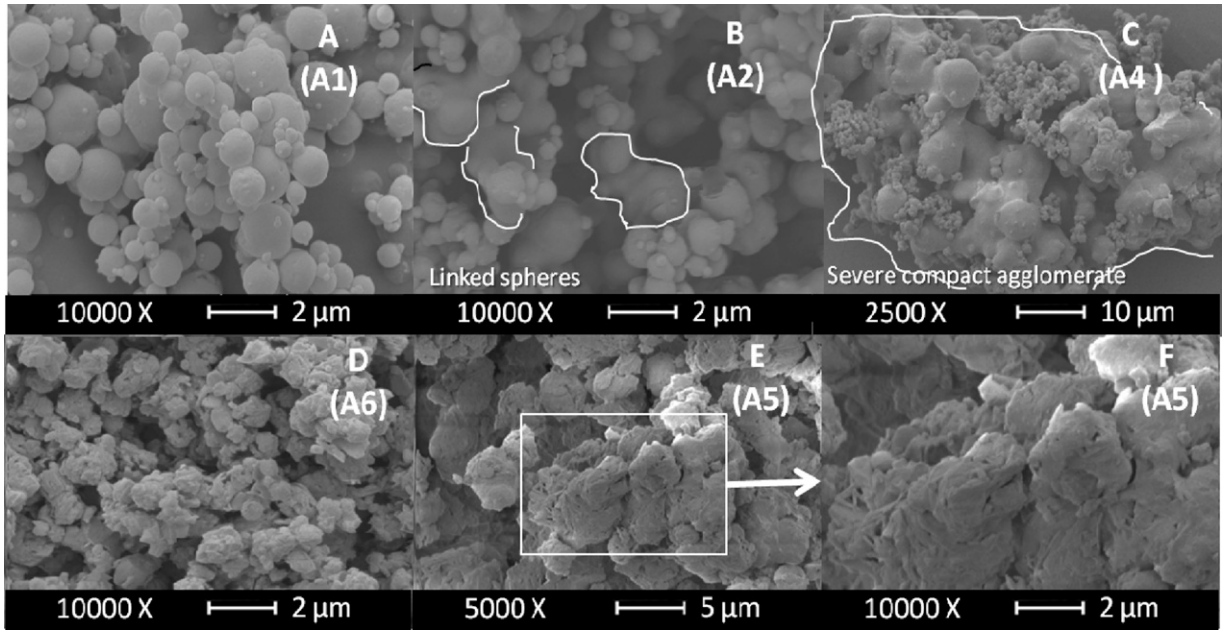

Fig. 3. SEM photographs of SD formulations (A1, A2, A4, A5 and A6) at magnifications of 2500×, 5000× and 10,000×. Formulation A1 (Fig. 3A) comprises individualized spheres. The ITZ liquid transition that occurred during the spray-drying of formulation A2 (outlet temperature of 60 °C) generated a linkage between spherical particles (Fig. 3B). This transition was exacerbated if the spray-dryer temperature was increased (formulation A4; outlet temperature 70 °C), which induced the formation of severe agglomeration upon cooling. Fig. 3D, E and F illustrate particle surface aspect modification when adding TPGS to the composition.

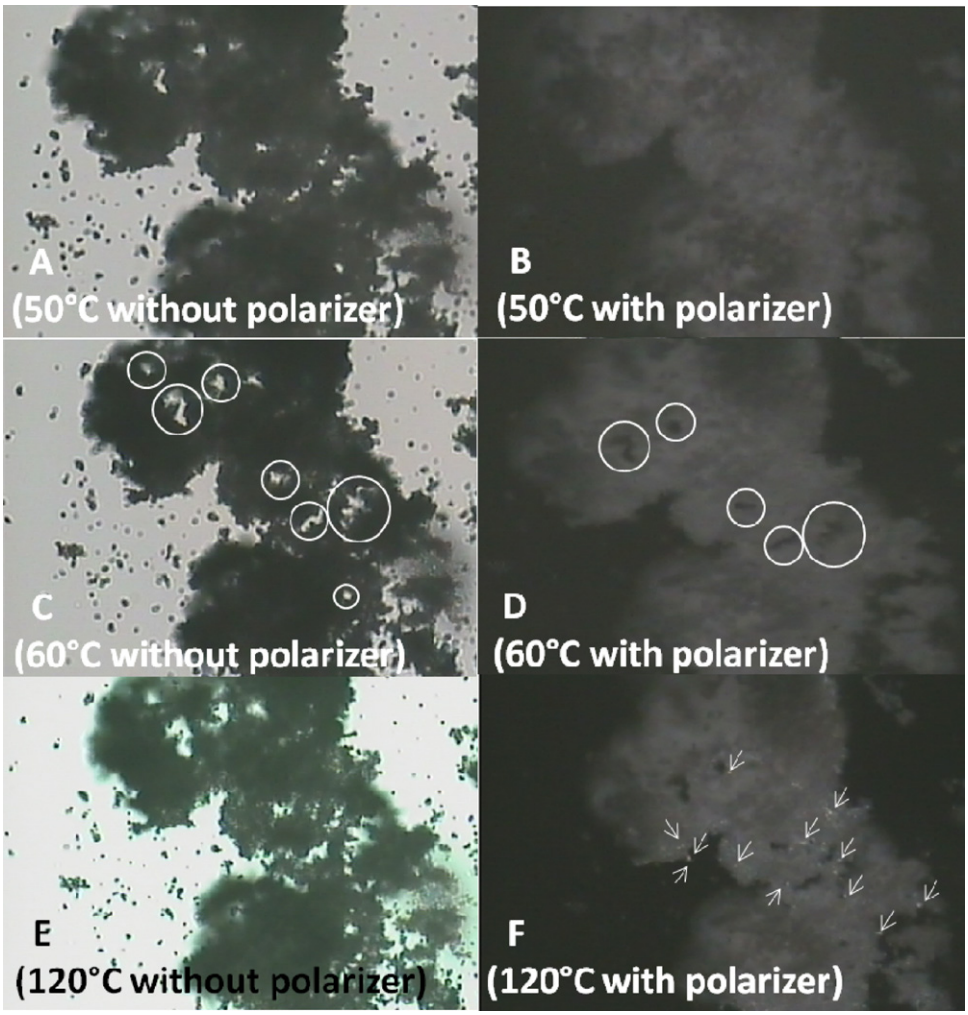

Fig. 4. HSM photographs (magnification of 200×) obtained for formulation A1. Each image was taken with and without a polarizer, which is used to detect crystalline phases. Samples were heated from 50 °C to 90 °C per steps of 5 °C maintained during 60 min (after each increment) follow by a continuous heating from 90 to 180 °C at a rate of 5 °C/min. Fig. 4C and D illustrates (white circles) the visual modification observed while maintaining the sample at 60 °C due to ITZ transition into liquid crystal. Recrystallized ITZ fractions are visible under polarized light when increasing temperature up to 105 °C. ITZ crystals intensity reached a maximum at 120 °C (white arrows, Fig. 4F).

deposited in the upper stages of 79.7% and 52.8% in comparison of a $D[4.3]$ of $1.00 \pm 0.04\,\mu m$, a MMAD of $1.61 \pm 0.05\,\mu m$ and a percentage deposited in the upper stages of 11.2% for formulation A1 (without TPGS) (Table 3). The percentage of powders deposited in the upper stages of the impactor represents the proportion of particles that would be stopped in the oropharyngeal region after inhalation by a patient and that would be removed by mucociliary clearance from trachea or by swallowing in the throat. This proportion is then not part of the dose that could be active in the lung or absorbed to the systemic compartment through pulmonary mucosa.

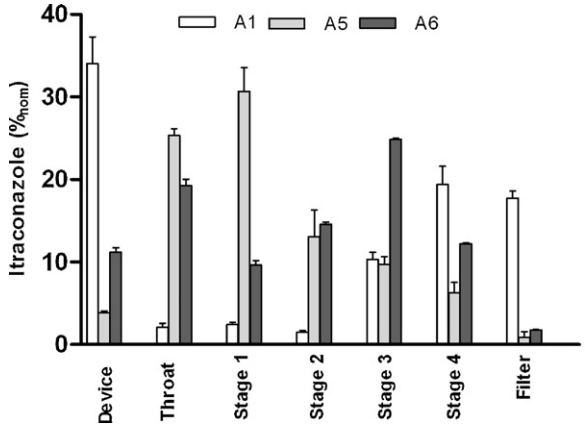

Fig. 5. Graphical representation of *in vitro* pulmonary deposition patterns of SD ITZ formulations A1, A5 and A6 (MsLI, 100 L/min, 2.4 s, $n = 3$). ITZ doses recovered from the device, the throat and stages 1–5 of the MsLI deposition are expressed as a % of the nominal dose (2.5 mg).

Regarding the aerodynamic assessment of fine particles and as expected from size analysis results, the FPF of formulation A5 (16%) was much lower than the FPFs of formulations A1 and A6 (47% and 37.2%, respectively). The last two formulations showed respectable aerosol performances.

Device and capsule retention of formulation was considerably reduced when TPSG was introduced into the formulations (the emitted doses were 85.9%, 82.5% and 53.3% for formulations A5, A6 and A1, respectively). This may have been influenced by different particle surface properties that reduced surface cohesion. On one hand, the smaller particle size and smoother surfaces of formulation A1, compared to formulations A5 and A6, enhanced the total surface area of particles, which generated greater surface interaction with the capsule and device and greater particle cohesion. On the other hand, the TPGS in formulation A5 and A6 could have had a lubricant effect that improved device and capsule emptying.

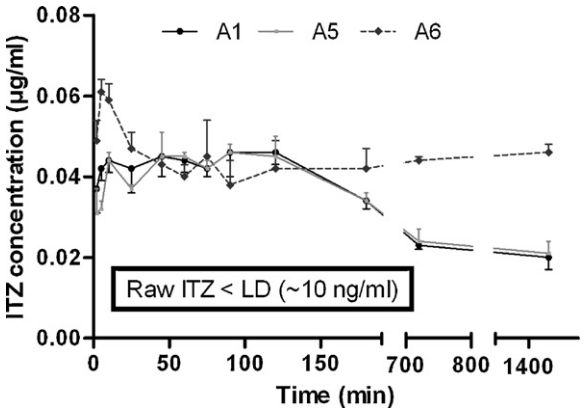

Fig. 6. Saturation solubility profiles of formulation A1 (•, solid black line), formulation A5 (■, solid grey line) and formulation A6 (♦, dashed grey line) in physiological phosphate buffer with 0.02% DPPC set at pH 7.2 and 37 °C at supersaturation conditions (mean ± S.D., $n = 3$). The raw ITZ saturation solubility was below the detection limit of the HPLC-UV quantification method (<10 ng/ml).

3.4. *In vitro* solubility/dissolution characteristics

For drugs acting locally in the lung, such as inhaled ITZ in the case of an invasive pulmonary fungal infection, the principal aims are to maximize drug lung concentration and residence time while minimizing the systemic concentration to reduce systemically mediated adverse events or interactions (McConville et al., 2006). Once inhaled, ITZ drug particles will be deposited on lung surfaces covered with lung surfactant, and (partial) drug dissolution will occur within this fluid. The extent of the active ingredient that is dissolved will therefore determine the fraction of drug that will be available to perform its pharmacological activity. This fraction of dissolved inhaled particles will also be subject to the absorption process. The undissolved drug fraction will also be progressively removed from the lungs by macrophage phagocytosis in the alveolar region and mucociliary/cough clearance in the conduction airways. The latter two mechanisms will progressively reduce the drug lung concentration and consequently reduce the potential action of the drug within the lungs. The ITZ saturation solubility in SLF is extremely low (~8 ng/ml; Yang et al., 2010). *In vivo*, this may lead to (i) very low availability of ITZ in the lung fluid surrounding the dry drug particles (ii) excessive non-absorptive clearance defense mechanism which may both considerably reduce the available drug concentration in the lungs and residence time (Mobley and Hochhaus, 2001). Thus, one major objective of our ITZ-based DPI formulations was to enhance the ITZ saturation solubility and dissolution rate to allow a greater available drug fraction to be obtained and to reduce non-absorptive clearance mechanisms.

The saturation solubility kinetic analysis showed that formulations A1, A5 and A6 provided greater saturation levels (4- and 6-fold greater) in the physiological phosphate buffer (pH 7.2, 37 °C) containing 0.02% (w/v) DPPC than the unformulated drug (Table 2 and Fig. 6). Indeed, raw ITZ was analyzed under the same conditions, but no detectable signals throughout the test allowed its saturation solubility to be estimated. ITZ saturation solubility was therefore considered to be below the detection limit of the analytical method (i.e., 10 ng/ml), which is consistent with the reported saturation solubility of ITZ in SLF (8 ng/ml; Yang et al., 2010).

Formulations A1 and A5 showed very similar saturation kinetic profiles with a maximum value of 46 ng/ml after 90 min and a decrease of up to 20 ng/ml after 24 h. Formulation A6 supersaturated more quickly and to a greater extent, with a maximum solubility of 61 ng/ml after 5 min and a saturation solubility of 46 ng/ml after 24 h. The latter formulation provided a greater saturation solubility that was reached more quickly than the other two formulations. As shown previously, in all formulations, ITZ was in an amorphous glassy state. This form of ITZ possesses a higher dissolution rate than the respective crystalline form (Six et al., 2004), probably due to greater saturation solubility, which allowed the formulations to form supersaturated solutions. During the saturation tests, these solutions progressively decreased to a lower equilibrium solubility because the remaining glassy ITZ particles in contact with the dissolution medium recrystallized into a lower-energy, more stable form that possesses a lower saturation solubility (Freiwald et al., 2005). The apparition of ITZ crystals throughout the test was observed under polarized light microscopy. This apparition prevented the attainment of the maximum reachable equilibrium solubility of amorphous ITZ particles in suspension and the dissolution medium. As mentioned previously, the saturation solubility value of formulation A6 was superior to the values obtained for formulations A1 and A5. Thus, the TPGS may have reduced the re-crystallization of ITZ amorphous particles in suspension by intermolecular interactions that allow attainment of a greater saturation solubility. Intermolecular interactions between polymers and amorphous drugs that prevent recrystallization in solution have already been reported, but the exact mechanisms are not clear (Murdande et al., 2011). However, formulation A5, containing the same TPGS/ITZ ratio as formulation A6 (10% TPGS, expressed in terms of the weight of ITZ), exhibited lower solubility enhancement. Despite this ratio, the TPGS in formulation A5 did not reduce recrystallization. However, formulation A6 had better wettability, which may explain this difference. Indeed, formulation A6, which contained 9.8% ITZ, is less hydrophobic than formulation A5 (with an ITZ content of 34.6%), which allowed better wettability and therefore quicker supersaturation onset. In addition, as previously seen, the TPGS had a tendency to accumulate on particle surfaces after spray-drying for solutions with a high proportion of TPGS, as demonstrated by Kawakami et al. (2010). This tendency may have reduced the quantity of TPGS inside formulation A5 that could 'intimately' protect amorphous ITZ from re-crystallization, leading to a direct decrease in solubility compared to formulation A6.

In comparison with raw ITZ, these formulations should provide higher dissolved ITZ concentrations *in vivo* in the lining lung fluid. These higher drug concentrations may enhance therapeutic activity because of a possible greater amount of diffused "active drug" in the fungal infiltration. However, this fraction would also be rapidly removed from the lung to the systemic compartment by diffusion due to the high tissue permeation of ITZ, which is why the dissolution profile of the DPI formulations must be evaluated in sink conditions. Faster dissolution rates would correlate with a faster turnover of the amount of API that would be lost secondary to the absorptive clearance that would occur in the lining fluid. The *in vitro* drug release profiles of the raw ITZ and formulations A1, A5 and A6 were evaluated under sink conditions (pH 1.2; 0.3% SDS; Fig. 7). Each formulation presented a significantly different dissolution profile ($f_2 < 50$) and a faster dissolution rate compared to raw ITZ (MDT of 62.1 min, 50.4 min, 49.6 min and 37.9 min for micronized raw ITZ and formulations A1, A5 and A6, respectively). The SD of ITZ prepared using only mannitol (formulation A1) accelerated the ITZ dissolution rate significantly ($f_2 = 40.92$; MDT of 62.1 min and 50.4 min for raw ITZ and formulation A1, respectively). Because the dissolution of a drug compound is directed by three major physicochemical properties – saturation solubility, the particles' surface area, and wetting properties – the enhanced dissolution rate observed for formulation A1 was explained by the combination of the SD formation and drug amorphization. Indeed, on one hand, we showed that the SD formation of glassy ITZ with mannitol provided greater ITZ saturation solubility than the raw crystalline form. On the other hand, once in contact with the dissolution medium, the mannitol from the formulations was quickly dissolved, leaving amorphous ITZ particles with improved solubility that were

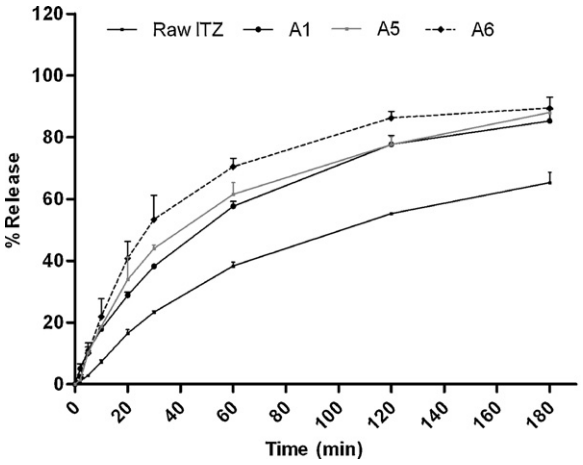

Fig. 7. Dissolution release profiles (mean ± S.D., $n = 3$) of ITZ from the DPI formulations (A1, A5 and A6) and the raw ITZ. These profiles were determined after impaction (NGI with an Axahaler® device at 60 l/min, 4 s, and one N°. 3 HPMC capsule) of a quantity of particles corresponding to 600 μg of ITZ (stage 3, d_{ae} from 2.82 to 4.46 μm) on a removable insert placed into the vessel of the USP 33 type II dissolution apparatus (300 ml of dissolution medium at pH 1.2, 37 °C, paddle operating speed 75 rpm).

probably in a very fine divided state that also accelerated the ITZ dissolution rate by enhancing the surface area that was available to the dissolution medium. Formulation A6 showed the fastest dissolution velocity, with an MDT of 37.9 min. This effect probably resulted from the combination of (i) drug particle wetting enhancement due to lower ITZ content and the surfactant-type activity of TPGS and (ii) the greater saturation solubility, which is beneficial in terms of dissolution. Formulation A1 showed the slowest dissolution velocity, with an MDT of 50.4 min that was probably due to lower saturation solubility and the lack of TPGS, which enhances the wetting of amorphous particles. Indeed, despite the same saturation solubility, formulation A5 showed a slightly faster release profile than formulation A1 (MDT of 49.6 min *vs.* 50.4 min for formulation A1; Fig. 7) due to the presence of TPGS, which allowed better hydrophobic ITZ wettability and therefore enhanced the dissolution rate.

4. Conclusion

We successfully demonstrated that the formation of matricial mannitol SD microparticles in which a poorly water-soluble API, ITZ, was dispersed in an amorphous state offered improved dissolution rate and saturation solubility compared to bulk ITZ while providing good aerosolization properties. The dry powders were produced by a simple spray-drying method using only low-potential toxicity solvents (USP class III) and excipients. The use of a conjugated-polymeric surfactant (TPGS) was beneficial in terms of the dissolution rate and saturation solubility. However, it limited particle aerosol performance, mainly due to its surface accumulation and its softening during the spray-drying process, which both decreased the respirable fraction by increasing particle size and limited dissolution improvement by reducing the TPGS available inside the dried particles. The reduction of ITZ content to 10% (w/w) in the SD while keeping an ITZ:TPGS ratio of 10% seemed to provide the formulation with the best solubility properties. This formulation concept could be envisaged to treat pulmonary invasive aspergillosis. The high saturation levels, the relatively fast dissolution rate and the high particle fractions should allow an adequate *in situ* pulmonary drug concentration (superior to the minimal inhibitory concentration of the mold) to be provided by maximizing the fraction of the drug that could diffuse and exercise its antifungal activity inside fungal lesions. Future pharmacokinetic studies (local and systemic) in the mouse will be conducted to evaluate the behavior of these systems *in vivo* in terms of drug dissolution, absorption and elimination after endotracheal insufflation.

References

Amidon, G.L., Lennernas, H., Shah, V.P., Crison, J.R., 1995. A theoretical basis for a biopharmaceutic drug classification—the correlation of in vitro drug product dissolution and in vivo bioavailability. Pharm. Res. 12, 413–420.

Blagden, N., de Matas, M., Gavan, P.T., York, P., 2007. Crystal engineering of active pharmaceutical ingredients to improve solubility and dissolution rates. Adv. Drug. Deliv. Rev. 59, 617–630.

Chang, C.H., Franses, E.I., 1995. Adsorption dynamics of surfactants at the air/water interface—a critical-review of mathematical-models, data, and mechanisms. Colloids Surf., A 100, 1–45.

Daviskas, E., Anderson, S.D., Jaques, A., Charlton, B., 2010. Inhaled mannitol improves the hydration and surface properties of sputum in patients with cystic fibrosis. Chest 137, 861–868.

Freiwald, M., Valotis, A., Kirschbaum, A., McClellan, M., Murdter, T., Fritz, P., Friedel, G., Thomas, M., Hogger, P., 2005. Monitoring the initial pulmonary absorption of two different beclomethasone dipropionate aerosols employing a human lung reperfusion model. Respir. Res., 6.

Goddeeris, C., Willems, T., Van den Mooter, G., 2008. Formulation of fast disintegrating tablets of ternary solid dispersions consisting of TPGS 1000 and HPMC 2910 or PVPVA 64 to improve the dissolution of the anti-HIV drug UC 781. Eur. J. Pharm. Sci. 34, 293–302.

Hickey, M.B., Peterson, M.L., Scoppettuolo, L.A., Morrisette, S.L., Vetter, A., Guzman, H., Remenar, J.F., Zhang, Z., Tawa, M.D., Haley, S., Zaworotko, M.J., Almarsson, O., 2007. Performance comparison of a co-crystal of carbamazepine with marketed product. Eur. J. Pharm. Biopharm. 67, 112–119.

Hoeben, B.J., Burgess, D.S., McConville, J.T., Najvar, L.K., Talbert, R.L., Peters, J.I., Wiederhold, N.P., Frei, B.L., Graybill, J.R., Bocanegra, R., Overhoff, K.A., Sinswat, P., Johnston, K.P., Williams, R.O., 2006. In vivo efficacy of aerosolized nanostructured itraconazole formulations for prevention of invasive pulmonary aspergillosis. Antimicrob. Agents Chemother. 50, 1552–1554.

Jones, R.M., Neef, N., 2012. Interpretation and prediction of inhaled drug particle accumulation in the lung and its associated toxicity. Xenobiotica 42, 86–93.

Kawakami, K., Sumitani, C., Yoshihashi, Y., Yonemochi, E., Terada, K., 2010. Investigation of the dynamic process during spray-drying to improve aerodynamic performance of inhalation particles. Int. J. Pharm. 390, 250–259.

Lian, Y., 2001. Amorphous pharmaceutical solids: preparation, characterization and stabilization. Adv. Drug Deliv. Rev. 48, 27–42.

Loftsson, T., Brewster, M.E., 2010. Pharmaceutical applications of cyclodextrins: basic science and product development. J. Pharm. Pharmacol. 62, 1607–1621.

McConville, J.T., Overhoff, K.A., Sinswat, P., Vaughn, J.M., Frei, B.L., Burgess, D.S., Talbert, R.L., Peters, J.I., Johnston, K.P., Williams, R.O., 2006. Targeted high lung concentrations of itraconazole using nebulized dispersions in a murine model. Pharm. Res. 23, 901–911.

Mobley, C., Hochhaus, G., 2001. Methods used to assess pulmonary deposition and absorption of drugs. Drug Discov. 6, 367–375.

Moss, O.R., 1979. Simulants of lung interstitial fluid. Health Phys. 36, 447–448.

Murdande, S.B., Pikal, M.J., Shanker, R.M., Bogner, R.H., 2011. Solubility advantage of amorphous pharmaceuticals, Part 3: is maximum solubility advantage experimentally attainable and sustainable. J. Pharm. Sci. 100, 4349–4356.

Pham, S., Wiedmann, T.S., 2001. Dissolution of aerosol particles of budesonide in Survanta (TM), a model lung surfactant. J. Pharm. Sci. 90, 98–104.

Pilcer, G., Amighi, K., 2010. Formulation strategy and use of excipients in pulmonary drug delivery. Int. J. Pharm. 392, 1–19.

Pilcer, G., Wauthoz, N., Amighi, K., 2011. Lactose characteristics and the generation of the aerosol. Adv. Drug Deliv. Rev., in press.

Polli, J.E., Rekhi, G.S., Augsburger, L.L., Shah, V.P., 1997. Methods to compare dissolution profiles and a rationale for wide dissolution specifications for metoprolol tartrate tablets. J. Pharm. Sci. 86, 690–700.

Porter, C.J.H., Trevaskis, N.L., Charman, W.N., 2007. Lipids and lipid-based formulations: optimizing the oral delivery of lipophilic drugs. Nat. Rev. Drug Discov. 6, 231–248.

Schulz, H., 1998. Mechanisms and factors affecting intrapulmonary particle deposition: implications for efficient inhalation therapies. Drug Discov. Today 1, 336–344.

Serajuddin, A.T.M., 1999. Solid dispersion of poorly water-soluble drugs: early promises, subsequent problems, and recent breakthroughs. J. Pharm. Sci. 88, 1058–1066.

Shah, A.R., Banerjee, R., 2011. Effect of D-alpha-tocopheryl polyethylene glycol 1000 succinate (TPGS) on surfactant monolayers. Colloids Surf. B: Biointerfaces 85, 116–124.

Six, K., Verreck, G., Peeters, J., Binnemans, K., Berghmans, H., Augustijns, P., Kinget, R., Van den Mooter, G., 2001. Investigation of thermal properties of glassy itraconazole: identification of a monotropic mesophase. Thermochim. Acta 376, 175–181.

Six, K., Murphy, J., Weuts, I., Craig, D.Q.M., Verreck, G., Peeters, J., Brewster, M., Van den Mooter, G., 2003. Identification of phase separation in solid dispersions of

itraconazole and Eudragit (R) E100 using microthermal analysis. Pharm. Res. 20, 135–138.
Six, K., Verreck, G., Peeters, J., Brewster, M., Van den Mooter, G., 2004. Increased physical stability and improved dissolution properties of itraconazole, a class II drug, by solid dispersions that combine fast- and slow-dissolving polymers. J. Pharm. Sci. 93, 124–131.
Son, Y.J., McConville, J.T., 2009. Development of a standardized dissolution test method for inhaled pharmaceutical formulations. Int. J. Pharm. 382, 15–22.
Tran, C.L., Buchanan, D., Cullen, R.T., Searl, A., Jones, A.D., Donaldson, K., 2000. Inhalation of poorly soluble particles. II. Influence of particle surface area on inflammation and clearance. Inhal. Toxicol. 12, 1113–1126.
Van Eerdenbrugh, B., Vermant, J., Martens, J.A., Froyen, L., Van Humbeeck, J., Van den Monter, G., Augustijns, P., 2010. Solubility increases associated with crystalline drug nanoparticles: methodologies and significance. Mol. Pharm. 7, 1858–1870.
Vasconcelos, T., Sarmento, B., Costa, P., 2007. Solid dispersions as strategy to improve oral bioavailability of poor water soluble drugs. Drug Discov. Today 12, 1068–1075.
Wauthoz, N., Deleuze, P., Saumet, A., Duret, C., Kiss, R., Amighi, K., 2010. Temozolomide-based dry powder formulations for lung tumor-related inhalation treatment. Pharm. Res. 28, 762–775.
Yan, A., Dem Bussche, A., Kane, A.B., Hurt, R.H., 2007. Tocopheryl polyethylene glycol succinate as a safe, antioxidant surfactant for processing carbon nanotubes and fullerenes. Carbon 45, 2463–2470.
Yang, W., Johnston, K.P., Williams, R.O., 2010. Comparison of bioavailability of amorphous versus crystalline itraconazole nanoparticles via pulmonary administration in rats. Eur. J. Pharm. Biopharm. 75, 33–41.
Zhang, J., Wu, L.B., Chan, H.K., Watanabe, W., 2011. Formation, characterization, and fate of inhaled drug nanoparticles. Adv. Drug. Deliv. Rev. 63, 441–455.